Supporting information

Probing the Proton Exchange Kinetics of $BaZr_{0.1}Ce_{0.7}Y_{0.1}Yb_{0.1}O_{3-\delta}$ Ceramic Electrolyte by *Operando* Diffuse Reflectance Infrared Fourier Transform Spectroscopy

Yuqing Meng[1], Fan Liu[1]*, Meng Li[1], Zixian Wang[1,2], Hao Deng[1,2], Qian Zhang[1], Haixia Li[1], Wanhua Wang[1], Quanwen Sun[1], Joshua Gomez[1], Zeyu Zhao[1], Haiyan Zhao[3]*, Dong Ding[1]*

1. Energy & Environmental Science and Technology, Idaho National Laboratory, Idaho Falls, Idaho 83415, United States
2. Tim Taylor Department of Chemical Engineering, Kansas State University, Manhattan, KS 66506, USA
3. Chemical and Biological Engineering Department, The Critical Materials and Energy Systems Innovation Center (CMESIC), University of Idaho, Idaho Falls, ID 83401, USA

*Corresponding authors: fan.liu@inl.gov (F.L.); haiyanz@uidaho.edu (H.Z.); dong.ding@inl.gov (D.D.)

Contents

Materials and Methods

The $BaZr_{0.1}Ce_{0.7}Y_{0.1}Yb_{0.1}O_{3-\delta}$ (BZCYYb1711) powders were synthesized via a solid-state reactive sintering (SSRS) method using commercial precursors: $BaCO_3$ (Alfa Aesar, 99.8%), CeO_2 (Alfa Aesar, 99.9%), ZrO_2 (Alfa Aesar, 99.7%), Y_2O_3 (Alfa Aesar, 99.9%), and Yb_2O_3 (Alfa Aesar, 99.9%). Stoichiometric amounts were weighed and homogenized in a Nalgene bottle using ball milling at 300 rpm for 24 h. The dried mixture was pressed into pellets and calcined at 1100°C in air for 5h. The resulting pellets were crushed and milled again in ethanol, followed by a second calcination to ensure phase purity. The final powders were used to fabricate green tapes for half-cell preparation.

Tape casting was used to prepare both hydrogen electrode and electrolyte layers. For the hydrogen electrode, NiO and BZCYYb17111 powders were mixed at a 6:4 weight ratio and ball-milled in an ethanol:toluene solvent for 24 h. Polyvinyl butyral (binder), butyl benzyl phthalate (plasticizer), and fish oil (dispersant) were added and ball-milled for an additional 24 h to achieve suitable rheology. The green tape was cast to a thickness of ~1 mm and dried at 38 °C for 4 h. Electrolyte tapes were similarly cast to a final thickness of ~80 μm. The electrode support and electrolyte layers were laminated together at 70 °C under a pressure of 4 tons for 5 h to form half-cell green tapes. After punching 1.27 cm (0.5 in) diameter disks, the laminates underwent pre-sintering at 920 °C to remove organic components. Final densification of the electrolyte was achieved by sintering at 1450 °C for 5 h in air. Electrical contact was achieved by painting a thin layer of silver paste onto both electrodes, followed by attaching silver wires for external connection. Then the ceramic cells were dried at 200 °C for 30 minutes to ensure good adhesion and electrical continuity. The electrode silver pattern was intentionally designed to provide reliable electrical contact while leaving the central electrolyte surface fully exposed to the infrared beam. The dimensions of the painted silver region have been well labeled in Figure S1c.

The ceramic cells (10 mm in diameter, Figure 1) were sealed using a ceramabond paste (Aremco Ceramabond 552) to ensure gas tightness at elevated temperatures. A K-type thermocouple was positioned within 1 cm beneath the cell to monitor and maintain uniform temperature distribution during measurements. The temperature was heated from room temperature to 600 °C at a rate of 2 °C min^{-1}, followed by ~2 h hold to allow complete curing and bonding of the seal. To verify the sealing quality, the open-circuit voltage (OCV) was continuously monitored during the initial reduction process (Figure S1d).

Operando DRIFTS were collected under both open-circuit voltage (OCV) and applied to external potential conditions. The flow rates of H_2 and air to the electrolyte and hydrogen electrode were maintained at 5 sccm and 50 sccm, respectively. Water vapor was introduced into the reactor using either an H_2O or D_2O bubbler (**Figure S1**). The Ni-based electrode side was first reduced in 5 sccm H_2 at 600 °C before conducting the DRIFTS and electrochemical measurements. A K-type thermocouple was positioned within 1 cm beneath the cell to monitor and maintain uniform temperature distribution during measurements. Flexible very high-temperature electrical-insulating mica sheets from McMaster-Carr was used to insulate circuit breakers and heating elements. The DRIFTS spectra were collected using a Thermo Scientific Nicolet iS50 FTIR spectrometer equipped with a customized Praying Mantis™ high temperature reaction chamber (Harrick Scientific Products). Spectra were recorded over the range of 4000–500 cm^{-1} with a resolution of 8 cm^{-1}, averaging 32 scans for each measurement to ensure a high signal-to-noise ratio. The background spectrum was collected using standard KBr powder prior to each experiment. This background was then subtracted from the sample spectra to remove system and

environmental contributions. During all DRIFTS measurements, the heating and cooling rates were controlled at around 2 °C min^{-1} to ensure thermal and ceramic cell stability. At each testing temperature, the system was stabilized for approximately 30 min before data collection to ensure thermal equilibrium. The phase of the ceramic electrolyte was characterized by X-ray diffraction (XRD, 2008 Bruker D8, CuKα) with a scan rate of 10 degree per minute at room temperature. The surface morphology of the electrolyte was examined using a scanning electron microscope (SEM, JEOL 6700F).

To enable direct comparison of the isotope exchange kinetics, the -OH and -OD intensities were normalized. Specifically, for each temperature and operating condition, the DRIFTS were collected as a function of time until the signal reached equilibrium. The maximum intensity of the -OH (or -OD) band at equilibrium was defined as 1, and all other spectra recorded during the transient process were normalized relative to this value. The resulting relative intensity (denoted as Rel. -OH or Rel. -OD) thus represents the ratio of the instantaneous intensity to the equilibrium intensity. This normalization approach allows consistent comparison across different temperatures and applied biases.

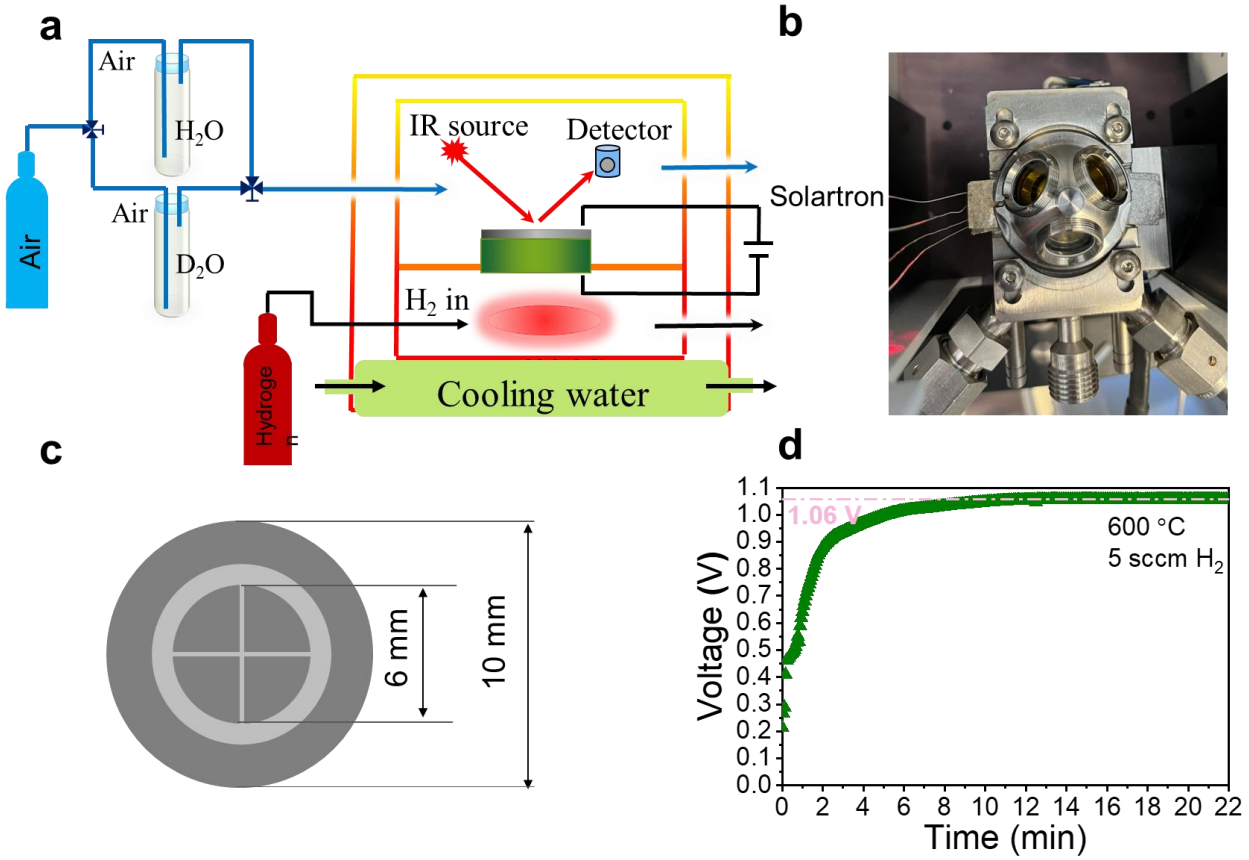

Figure S1. **(a)** Schematic illustration of the custom-built *operando* DRIFTS system. The setup features independent gas lines for H_2 and humidified air (H_2O or D_2O), a high-temperature heating stage, and an IR-transparent window for direct reflectance measurements; **(b)** Photograph of the assembled DRIFTS reaction cell showing the sealed configuration with the electrolyte-facing IR window exposed for real-time data acquisition. (**c**) The dimension of the ceramic cells used for DRIFTS experiments; (**d**) The reduction process of the single cell to verify the sealing and quality before DRIFTS measurement.

Note: This figure highlights the core innovation of this work: a temperature- and voltage-compatible DRIFTS platform for operando surface analysis under asymmetric electrochemical environments. The design allows precise control over gas composition, bias application, crucial for probing hydration dynamics under PCEC-relevant conditions. The electrode silver pattern was intentionally designed to provide reliable electrical contact while leaving the central electrolyte surface fully exposed to the infrared beam, and a stable OCV of around 1.06 V during reduction confirmed the integrity of both the seal and the ceramic cell prior to any testing.

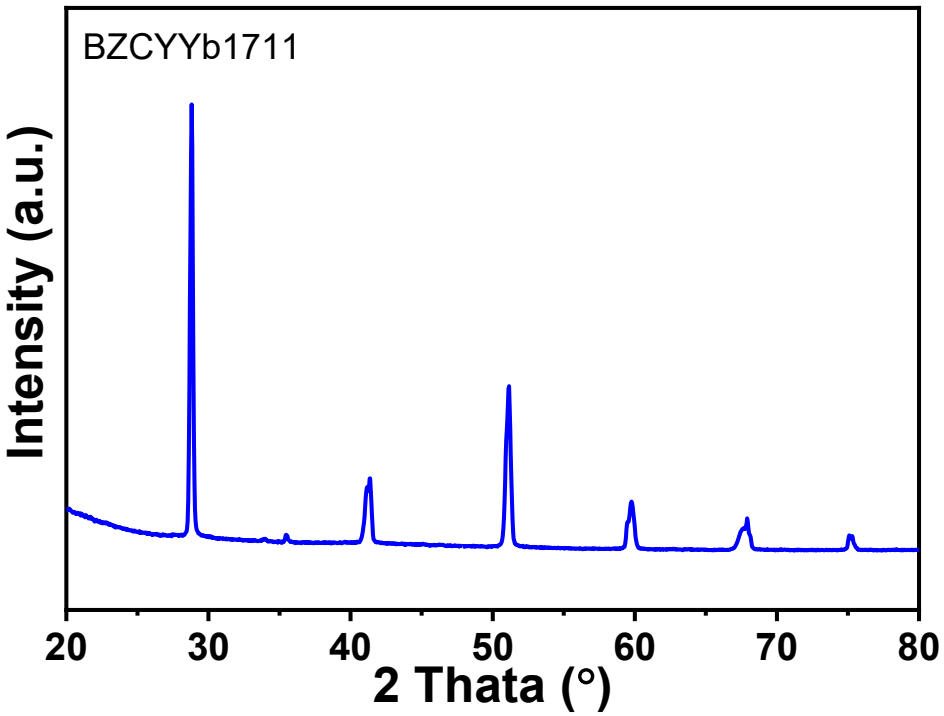

Figure S2. X-ray diffraction (XRD) pattern of the BZCYYb1711 electrolyte in the BZCYYb1711 | BZCYYb1711 + NiO half-cell after final sintering.

Note: XRD analysis confirms the formation of a single-phase BZCYYb1711 electrolyte after sintering, no second phase has been found.

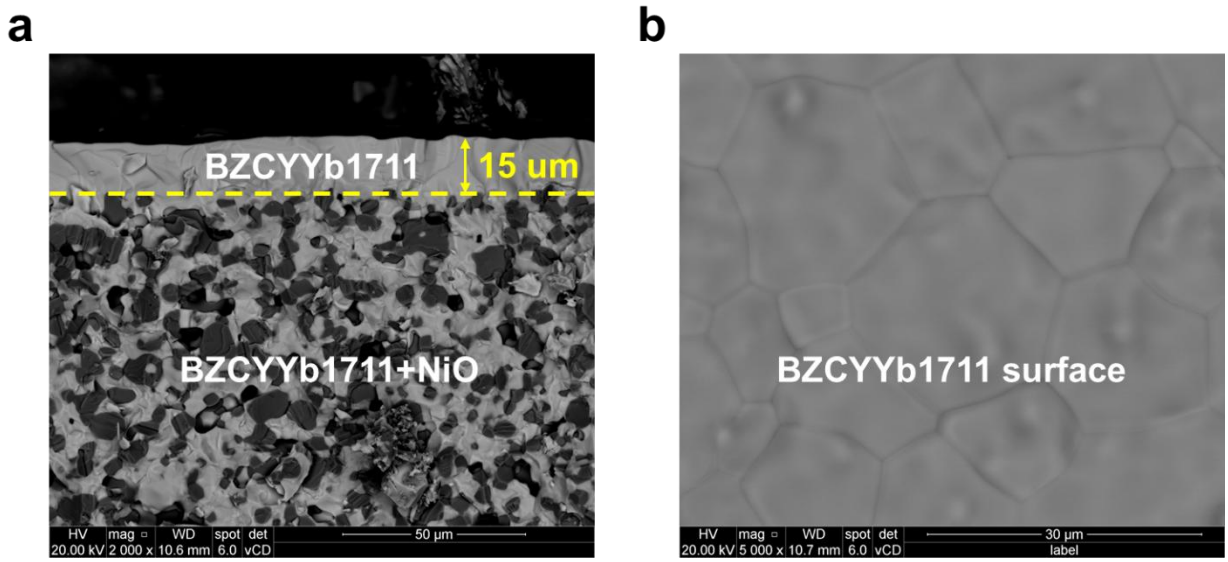

Figurer S3. **(a)** Cross-section of SEM image of BZCYYb1711 | NiO + BZCYYb1711 half-cell; **(b)** surface morphology of BZCYYb1711 electrolyte.

Note: A dense electrolyte layer with an approximate thickness of 15 µm was observed, exhibiting a uniformly dense surface morphology.

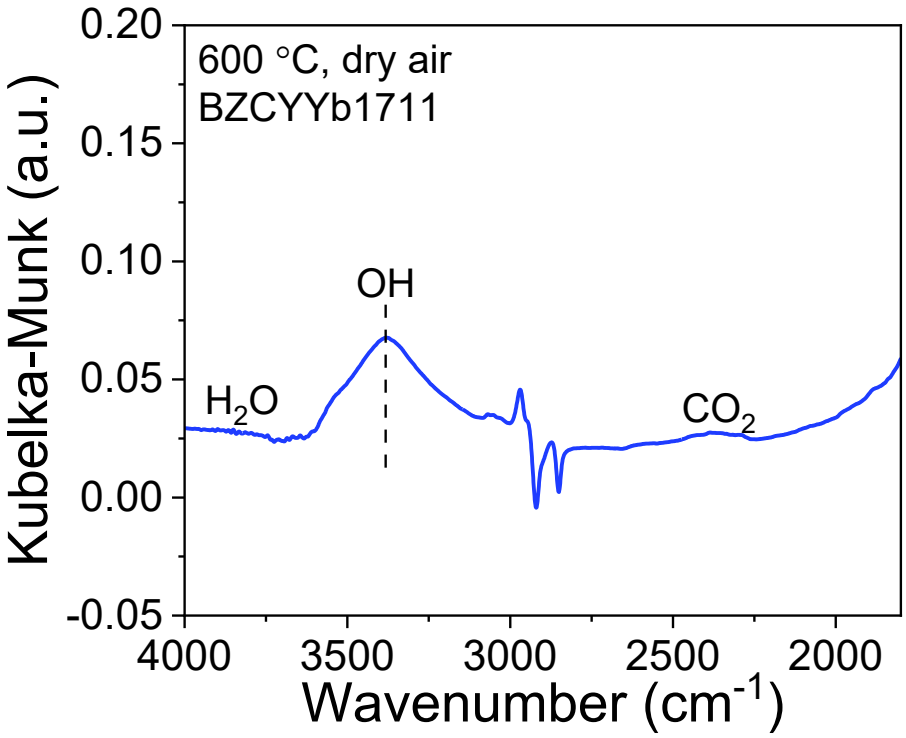

Figure S4. DRIFTS collected from the BZCYYb1711 electrolyte surface at 600 °C under dry air condition. The sample was pre-treated in dry air at 600 °C for at least 2 h to remove physiosorbed or weakly bound water.

Note: Despite the dry air environment, a strong O–H stretching band centered around 3380 cm^{-1} is observed, indicating the persistence of surface hydroxyl groups. This finding demonstrates the material's inherent hydration tendency. The observed -OH stretching bands on the electrolyte surface can originate from the strong intrinsic hydration ability of BZCYYb1711. During the cell manufacturing process, particularly during sintering and cooling in air, trace H_2O from feed lines, furnace tubes, and chamber walls can be incorporated, producing "built-in" hydration that leaves a population of surface-near -OH species, which can only be completely removed at much higher temperatures[1].

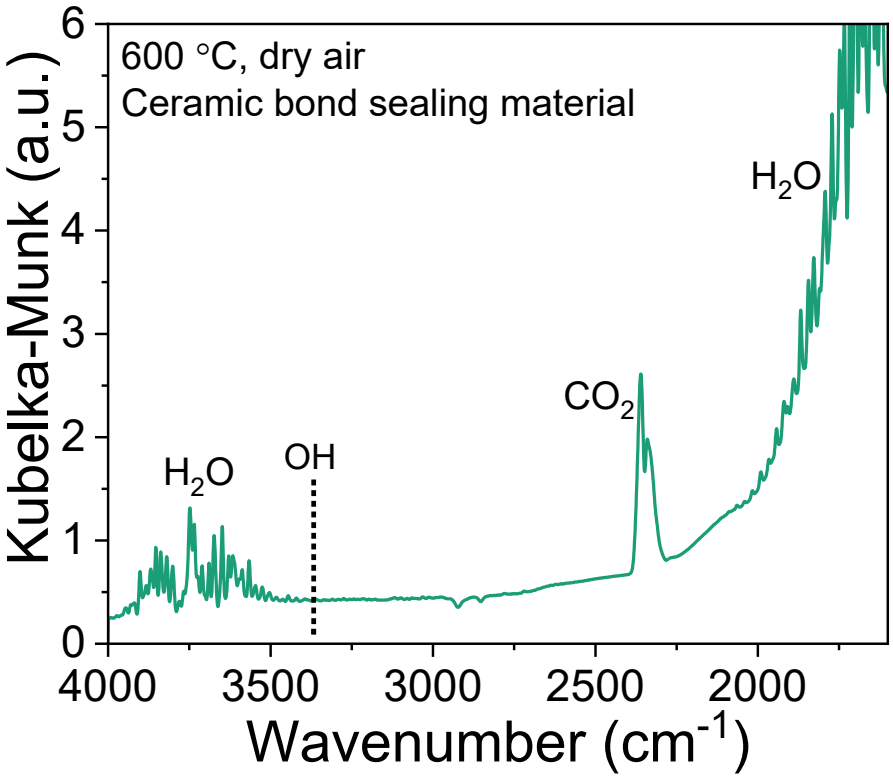

Figure S5. DRIFTS collected from the 552-ceramic bond (seal material) at 600 °C in dry air.

Note: No O–H stretching features are detected in the spectrum, indicating the 552-seal material is spectrally inactive in the relevant vibrational regions. This confirms that the O–H bands observed in DRIFTS experiments originate solely from the BZCYYb1711 electrolyte and not from external materials.

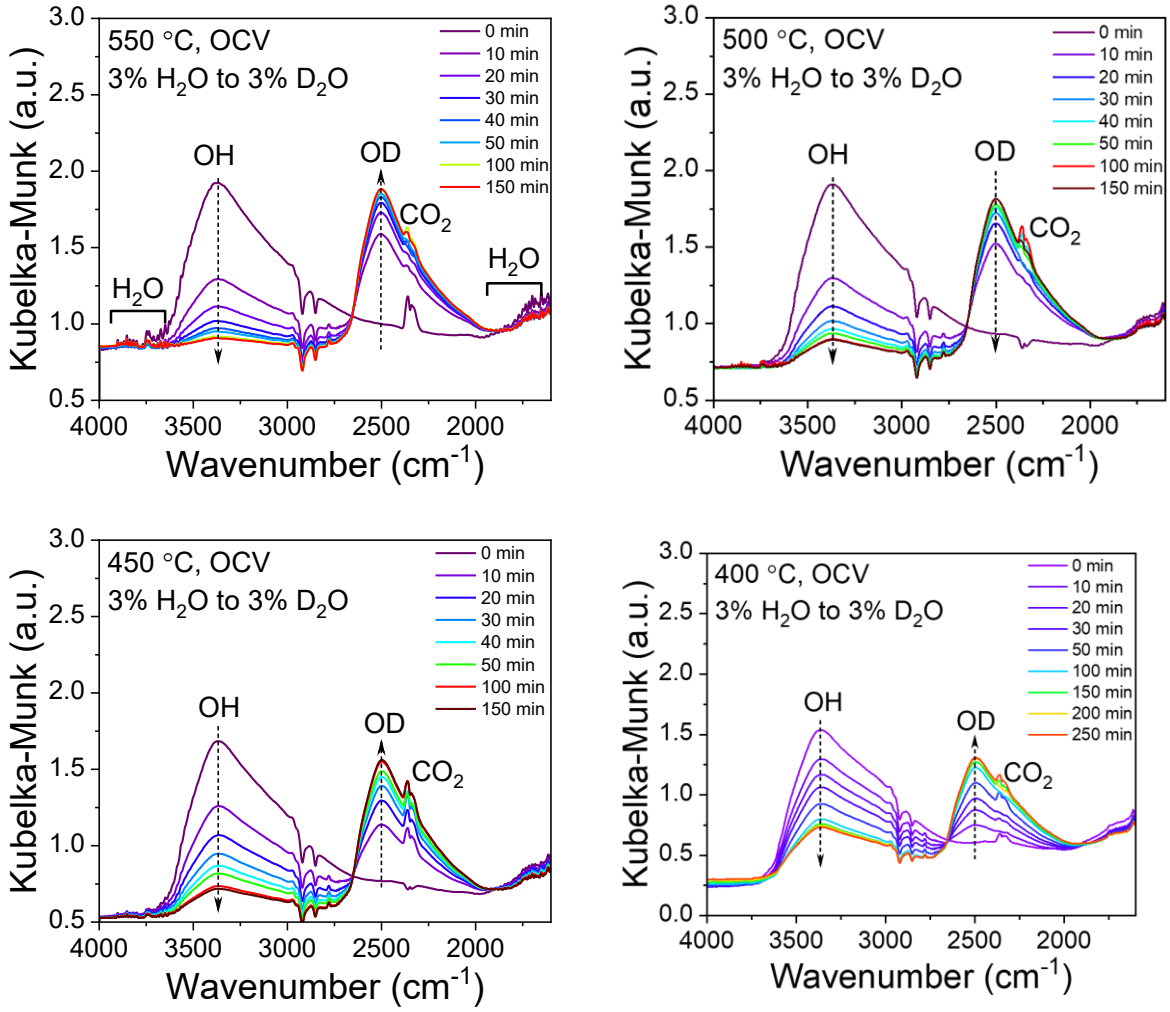

Figure S6. Time-resolved DRIFTS collected during isotope exchange from 3% H_2O-humidified air to 3% D_2O-humidified air at 550 °C-400 °C under OCV conditions.

Note: At all temperatures, the OH stretching band (~3379 cm^{-1}) gradually decreases, while a corresponding OD band (~2500 cm^{-1}) appears and intensifies, confirming that H/D isotope exchange occurs on the surface of the BZCYYb1711 electrolyte. The overall exchange process proceeds more slowly at lower temperatures, as visually indicated by the slower development of the OD signal. These observations are consistent with thermally activated surface processes.

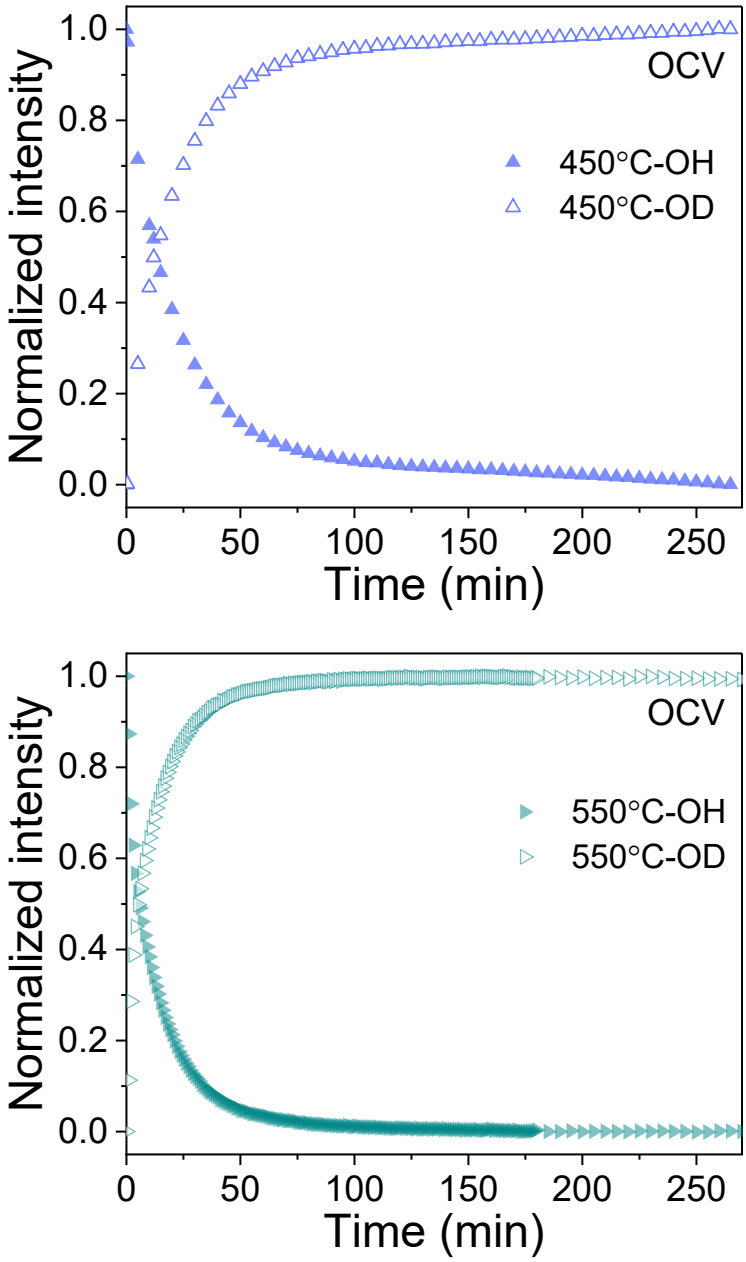

Figure S7. Normalized intensities of OH and OD bands over time during gas switching from 3% H_2O-humidified air to 3% D_2O-humidified air at 500 °C and 450 °C under OCV conditions.

Note: The OH signal progressively decreases while the OD intensity increases with time, reaching approximately equal values (~0.5 normalized intensity), which visually suggests symmetric exchange behavior. The transition is slower at 450 °C compared to 500 °C, consistent with thermally activated kinetics.

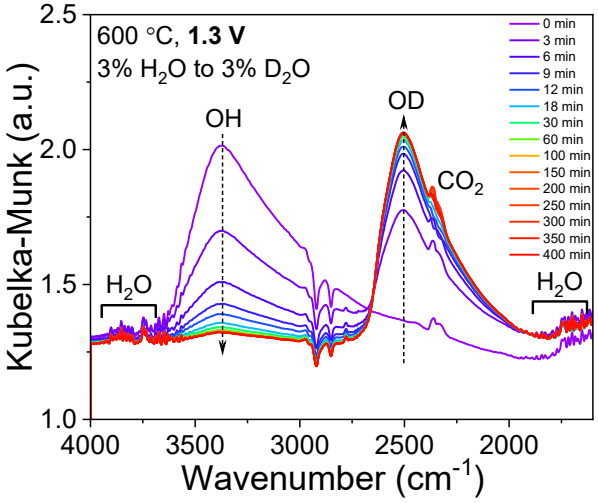
600 °C, 1.3 V
3% H2O to 3% D2O
0 min
3 min
6 min
9 min
12 min
18 min
30 min
60 min
100 min
150 min
200 min
250 min
300 min
350 min
400 min
OH
OD
CO2
H2O
H2O
Kubelka-Munk (a.u.)
Wavenumber (cm-1)

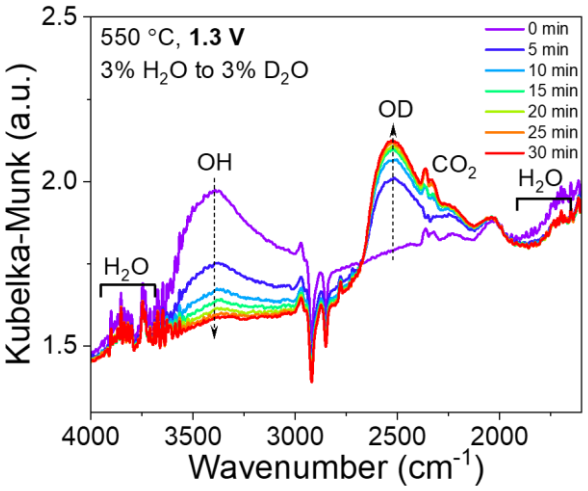
550 °C, 1.3 V
3% H2O to 3% D2O
0 min
5 min
10 min
15 min
20 min
25 min
30 min
OH
OD
CO2
H2O
H2O
Kubelka-Munk (a.u.)
Wavenumber (cm-1)

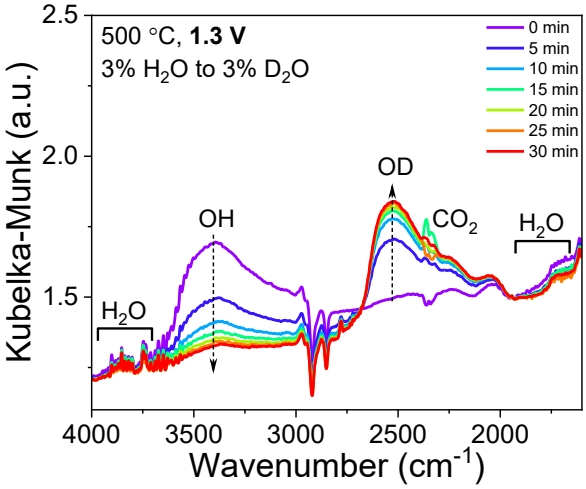
500 °C, 1.3 V
3% H2O to 3% D2O
0 min
5 min
10 min
15 min
20 min
25 min
30 min
OH
OD
CO2
H2O
H2O
Kubelka-Munk (a.u.)
Wavenumber (cm-1)

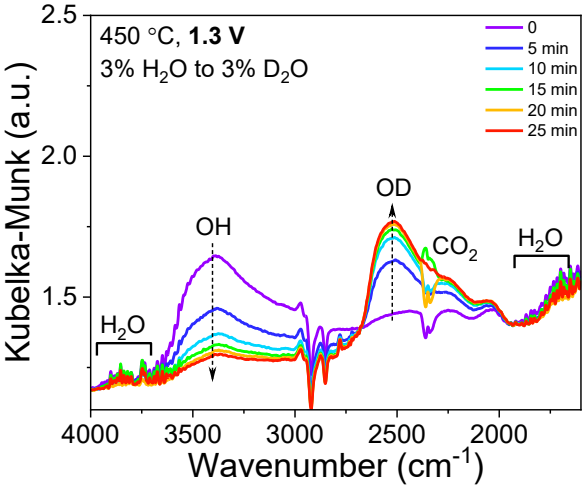
450 °C, 1.3 V
3% H2O to 3% D2O
0
5 min
10 min
15 min
20 min
25 min
OH
OD
CO2
H2O
H2O
Kubelka-Munk (a.u.)
Wavenumber (cm-1)

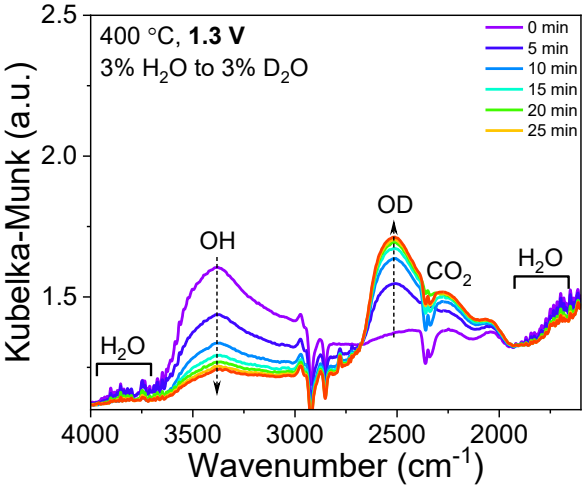
400 °C, 1.3 V
3% H2O to 3% D2O
0 min
5 min
10 min
15 min
20 min
25 min
OH
OD
CO2
H2O
H2O
Kubelka-Munk (a.u.)
Wavenumber (cm-1)

Figure S8. Time-resolved DRIFTS spectra collected during the gas switch from 3% H_2O-humidified air to 3% D_2O-humidified air at 600 °C-400 °C under a constant applied voltage of 1.3 V.

Note: The DRIFTS show a clear decay in the O–H stretching band (~3379 cm^{-1}) and simultaneous growth of the O–D band (~2500 cm^{-1}), indicating active H/D isotope exchange at the electrolyte surface. The transition occurs more rapidly at higher temperatures, consistent with thermally enhanced surface kinetics. Compared to OCV (see Figure S6), the exchange proceeds faster across all temperatures, confirming the accelerating effect of applied bias on hydration processes. These data support the conclusion that electrochemical potential lowers the energy barrier for surface proton exchange and enhances reaction rates.

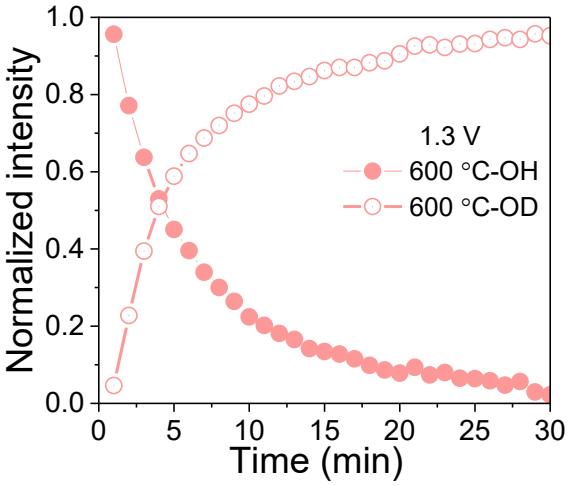
Normalized intensity
Time (min)
1.3 V
600 °C-OH
600 °C-OD

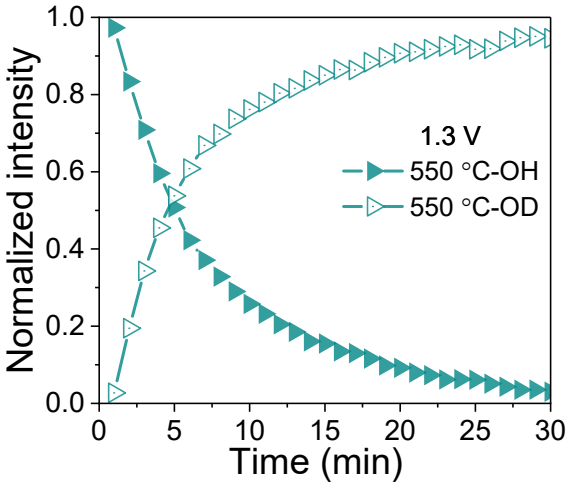
Normalized intensity
Time (min)
1.3 V
550 °C-OH
550 °C-OD

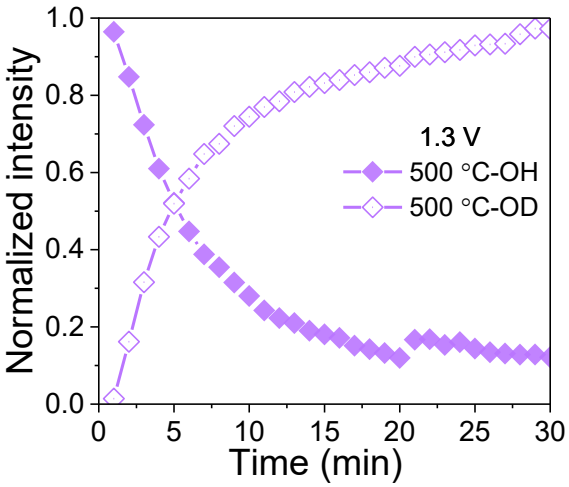
Normalized intensity
Time (min)
1.3 V
500 °C-OH
500 °C-OD

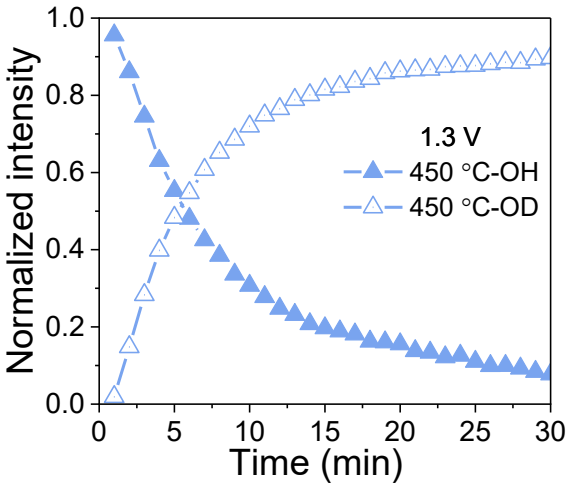
Normalized intensity
Time (min)
1.3 V
450 °C-OH
450 °C-OD

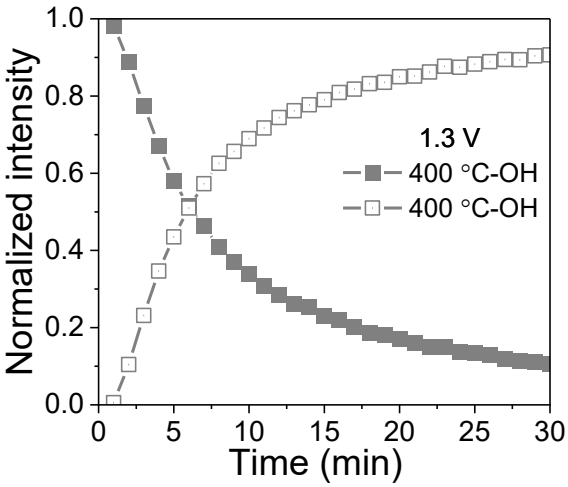
Normalized intensity
Time (min)
1.3 V
400 °C-OH
400 °C-OH

Figure S9. Normalized OH and OD band intensities over time during the gas switch from 3% H_2O-humidified air to 3% D_2O-humidified air at 600 °C-400 °C under an applied potential of 1.3 V.

Note: The OH intensity decreases while the OD intensity increases over time at all temperatures, reflecting the surface H/D isotope exchange process. The crossover point (normalized intensity ~0.5) occurs earlier at higher temperatures, qualitatively confirming that the exchange is thermally accelerated. Compared to OCV data (Figure S7), the exchange occurs more rapidly at each temperature, demonstrating that applied voltage facilitates proton removal and replacement by deuterium. These normalized plots visually highlight the impact of electrochemical bias on hydration kinetics and support the conclusion that surface exchange is strongly voltage-dependent in protonic ceramic electrolytes.

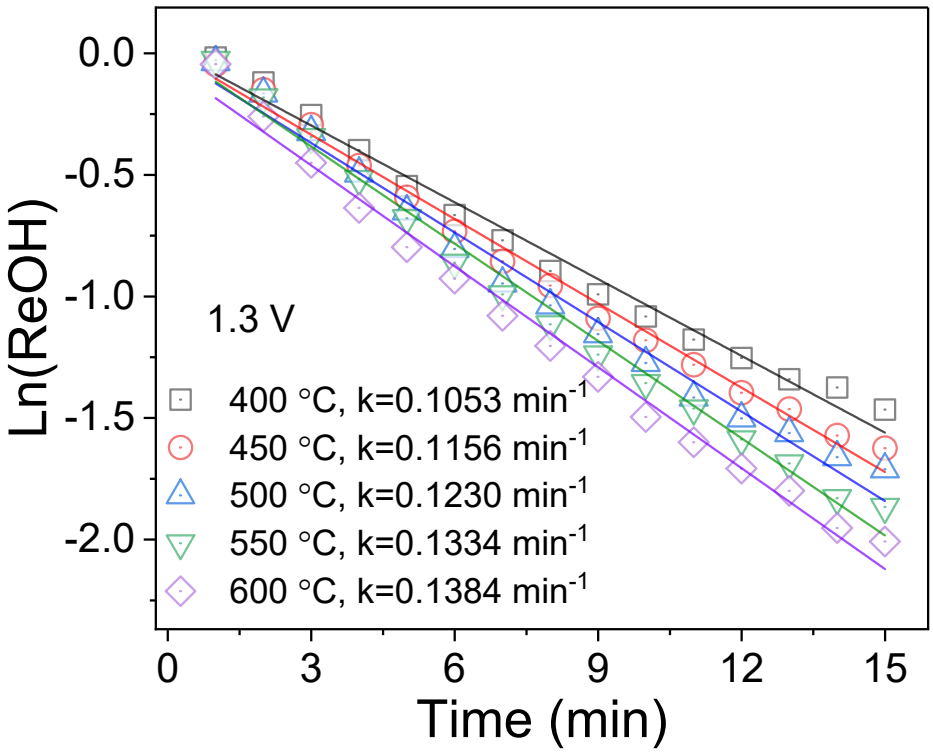

Figure S10. First-order kinetic plots showing the natural logarithm of the relative OH intensity [ln(Rel. OH)] as a function of time during the isotope exchange process (3% H_2O → 3% D_2O) at 400–600 °C under an applied potential of 1.3 V.

Note: The linear relationship between ln(Rel. OH) and time confirms that the surface isotope exchange process follows first-order kinetics with respect to surface hydroxyl coverage. The extracted rate increases systematically with temperature, ranging from k = 0.1053 min^{-1} at 400 °C to k = 0.1384 min^{-1} at 600 °C, consistent with thermally activated surface proton exchange. These quantitative results reinforce the conclusion that electrochemical bias significantly accelerates hydration kinetics and enable subsequent Arrhenius analysis for determining activation energies.

Reference:

(1) Hamze, L.; Joubert, O.; Quarez, E. Phase diagrams and chemical expansion upon hydration of proton conductors $BaZr_xCe_{0.8-x}Y_{0.1}Yb_{0.1}O_{2.9}(H_2O)_n$ ($0 \leq x \leq 0.8$; $0 \leq n \leq 0.1$). *J. Mater. Chem. A* **2025**, 10.1039/D5TA07218B. DOI: 10.1039/D5TA07218B.